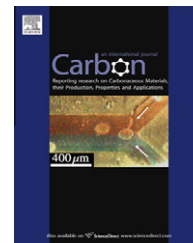


available at www.sciencedirect.comjournal homepage: www.elsevier.com/locate/carbon

Bulk growth of mono- to few-layer graphene on nickel particles by chemical vapor deposition from methane

Zongping Chen, Wencai Ren ^{*}, Bilu Liu, Libo Gao, Songfeng Pei, Zhong-Shuai Wu, Jinping Zhao, Hui-Ming Cheng ^{**}

Shenyang National Laboratory for Materials Science, Institute of Metal Research, Chinese Academy of Sciences, Shenyang 110016, PR China

ARTICLE INFO

Article history:

Received 23 January 2010

Accepted 26 May 2010

Available online 31 May 2010

ABSTRACT

A method for the bulk growth of mono- to few-layer graphene on nickel particles by chemical vapor deposition from methane at atmospheric pressure is described. A graphene yield of about 2.5% of the weight of nickel particles used was achieved in a growth time of 5 min. Scanning and transmission electron microscopy, Raman spectroscopy, thermogravimetry, and electrical conductivity measurements reveal the high quality of the graphene obtained. Suspended graphene can be prepared during this process, bridging the gaps between nearby nickel grains. After the growth of graphene the nickel particles can be effectively removed by a modest FeCl_3/HCl etching treatment without degradation of the quality of the graphene sheets.

© 2010 Elsevier Ltd. All rights reserved.

1. Introduction

Graphene, a new class of two-dimensional crystal only one atom thick, has attracted increasing interests due to its unique structure, peculiar physical properties and a wide range of promising applications [1–10]. In 2004, Novoselov et al. developed a simple method to fabricate graphene by mechanically splitting highly oriented pyrolytic graphite [1–5]. This method can provide graphene crystals with high structural and electronic quality for making proof-of-concept devices, but is not suitable for large-scale production of graphene because of its low yield [3]. Chemical exfoliation of graphite is widely considered to be an efficient method for large-scale production of graphene, which usually consists of the oxidation of graphite, exfoliation of graphite oxide, and reduction of the obtained graphene oxide [11–14]. However, the graphene obtained by this approach has poor quality, and hardly reaches its intrinsic properties due to the presence of oxygen-containing functional groups and structural defects introduced during the vigorous oxidation and exfoliation pro-

cesses [15]. Liquid-phase exfoliation of graphite is another promising method to produce graphene in a large quantity, but the graphene sheets may be damaged and cut into small pieces during the long time sonication process [16,17]. Different from the cleavage and exfoliation strategies, an alternative route is epitaxial growth of graphene layers on top of crystals such as SiC [18,19] and Ru [20]. However, the high cost of single crystal substrates and strict growth conditions significantly limit its applicability for large-scale production of graphene as well.

In 2008, Dato et al. developed a substrate-free gas-phase synthesis method to produce graphene sheets in a promising large quantity, but the graphene sheets produced by this process are usually small [21]. Recently, chemical vapor deposition (CVD) was developed to synthesize large-area mono- to few-layer graphene films on polycrystalline nickel films and copper foils [22–33]. The graphene film grown by this method exhibits high carrier mobility (up to $4000 \text{ cm}^2 \text{ V}^{-1} \text{ s}^{-1}$, close to that of mechanically cleaved graphene), very low sheet resistance, high optical transparency, and outstanding mechanical

^{*} Corresponding author: Fax: +86 24 2390 3126.

^{**} Corresponding author: Fax: +86 24 2390 3126.

E-mail addresses: wcren@imr.ac.cn (W. Ren), cheng@imr.ac.cn (H.-M. Cheng).

0008-6223/\$ - see front matter © 2010 Elsevier Ltd. All rights reserved.

doi:10.1016/j.carbon.2010.05.052

properties, suggesting its high quality and great potential for various applications [25,31]. For example, Kim et al. and Li et al. have demonstrated the macroscopic use of CVD-grown graphene in flexible, stretchable, and foldable electronics [25,34]. However, the yield of above-mentioned CVD-grown graphene is still low because of the limited growth area of flat metal substrates.

Considering the fact that graphene is grown from the surface of metal substrates, it is reasonable to expect that increasing the surface area of metal substrates could effectively improve the yield of graphene in CVD. In this work, we demonstrate the use of nickel particles, instead of flat nickel substrate, to realize the bulk growth of graphene sheets by CVD. A graphene yield of about 2.5% of the weight of nickel particles used was achieved within a CVD growth time of 5 min. Moreover, the graphene sheets obtained show excellent crystallinity, high thermal stability and good electrical conductivity. In addition, we found that the nickel particles after the growth of graphene can be easily removed by a simple etching process without degradation of the quality of the graphene sheets.

2. Experimental

2.1. CVD growth of graphene and removal of nickel particles

In our CVD, commercially available nickel particles of $\leq 30 \mu\text{m}$ in size were used to catalyze graphene growth. The nickel particles were first dispersed in ethylene glycol and then spread onto a Si/SiO₂ substrate, followed by drying in vacuum oven at 100 °C for 5 h. To further increase the yield of graphene, a certain quantity of nickel particles were placed directly in a quartz crucible. Then the nickel particles were put in a quartz tube with an outer diameter of 25 mm and heated to 1000 °C in a horizontal tube furnace (Lindberg Blue M, TF55030C) under Ar (500 sccm) and H₂ (200 sccm). After annealing for 5 min, a small amount of CH₄ (10 sccm) was introduced to initiate the growth of graphene at ambient pressure for 5 min. After growth, the furnace was cooled down to room temperature under the protection of Ar and H₂ at a cooling rate of 100 °C/min. To obtain pure graphene, the as-grown samples were treated in a FeCl₃ (1 M)/HCl (1 M) mixed aqueous solution to remove nickel particles, followed by filtration and thorough rinsing with deionized water [25].

2.2. Material characterization

The as-prepared and purified graphene were characterized by scanning electron microscopy (SEM, Nova NanoSEM 430, 15 kV, equipped with an X-ray energy dispersive spectrometer (EDS)), Raman spectroscopy (Jobin Yvon HR800, excited by 632.8 nm He–Ne laser with a laser spot size of $\sim 1 \mu\text{m}^2$), and transmission electron microscopy (TEM, Tecnai F30, 300 kV). For TEM specimen preparation, the purified graphene sheets were first sonicated in N-methylpyrrolidone (NMP) or ethanol for 30 min to form a homogeneous suspension, then the obtained solution was dropped onto a TEM grid. Thermogravimetry/derivative thermogravimetry (TG/DTG, Netzsch-STA

449C) of the purified sample were measured from 30 to 1000 °C at a heating rate of 10 °C/min in air to determine the thermal stability of the purified graphene.

2.3. Electrical conductivity measurements

To measure the electrical conductivity of our graphene, the above homogeneous suspension of graphene was dropped onto Au electrode arrays followed by drying in a vacuum oven at 100 °C for 5 h to remove the solvent and improve the contact between graphene and electrode. The Au electrode arrays used in the present study were prepared by standard photolithography [35,36], with a gap of 1 μm between the two electrodes. The current–voltage (*I*–*V*) curves of the graphene devices were measured with an electrochemical workstation instrument (CHI630C) at room temperature in ambient condition.

3. Results and discussion

The representative SEM images of the as-grown graphene are shown in Fig. 1. It can be found that all the nickel particles are wrapped by graphene films after CVD, indicating the high efficiency of this process for the bulk growth of graphene. Due to the increased surface area of nickel particles compared to a flat substrate (Fig. 1a), much more graphene sheets can be obtained within the same growth time. Similar to the growth of graphene on a flat substrate, most of the graphene films adhere to the surface of nickel particles with many wrinkles in graphene layers (Fig. 1b) [23]. Interestingly, we also found many suspended graphene films bridging the gaps of hundreds of nanometers between nearby nickel grains (Fig. 1c and d and Fig. S1 in Supplementary data), which has also been observed in graphene grown on flat substrates [24,31]. This phenomenon reveals that the graphene could grow with a similar behavior to carbon nanotubes (CNTs), which implies the possibility for the continuous growth of large-area suspended graphene by CVD. Furthermore, such suspended graphene sheets are free from the influence of substrates, and may be suitable for the investigation of the intrinsic properties of graphene [37]. For example, Bolotin et al. demonstrated that suspended single layer graphene exhibits an ultrahigh mobility in excess of 200,000 cm² V⁻¹ s⁻¹ at the electron density of $\sim 2 \times 10^{11} \text{cm}^{-2}$, which is significantly higher than that supported on a substrate [7]. Considering the similar growth conditions, we believe that the growth of graphene on nickel particles is similar to that of graphene on flat nickel surface, which is promoted by non-equilibrium segregation or precipitation of dissolved carbon upon cooling down, and the wrinkles are formed due to the difference in thermal expansion between graphene and nickel substrates [22,23].

After CVD growth, the nickel particles were removed efficiently by etching in FeCl₃ (1 M)/HCl (1 M) aqueous solution, and the resulting product is shown in Fig. 2a and b. Once the nickel particles are removed, the graphene films collapse and aggregate to each other, forming a curved and crumpled structure. EDS spectra of the graphene samples before and after etching are shown in Fig. 2c and d. It is evident that no nickel signals are found after etching (Fig. 2d), indicating that

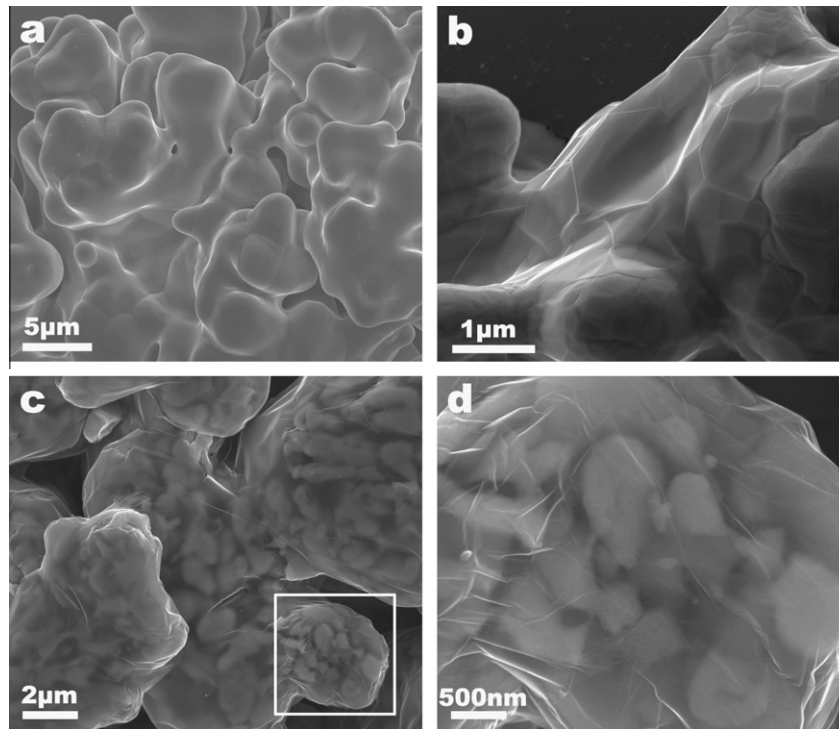


Fig. 1 – SEM images of the as-grown graphene on nickel particles by CVD. (a) Nickel particles annealed at 1000 °C for 5 min before CVD growth, showing that the particles have rich surface area. (b) Nickel particles after CVD growth, showing that the graphene films adhere to their surface with many wrinkles within the graphene layer. (c) Low-magnification SEM image of suspended graphene films wrapped around the nickel particles. (d) High-magnification SEM image of the square region in panel c, indicating a transparent suspended graphene film floating across the gaps between the nearby nickel grains.

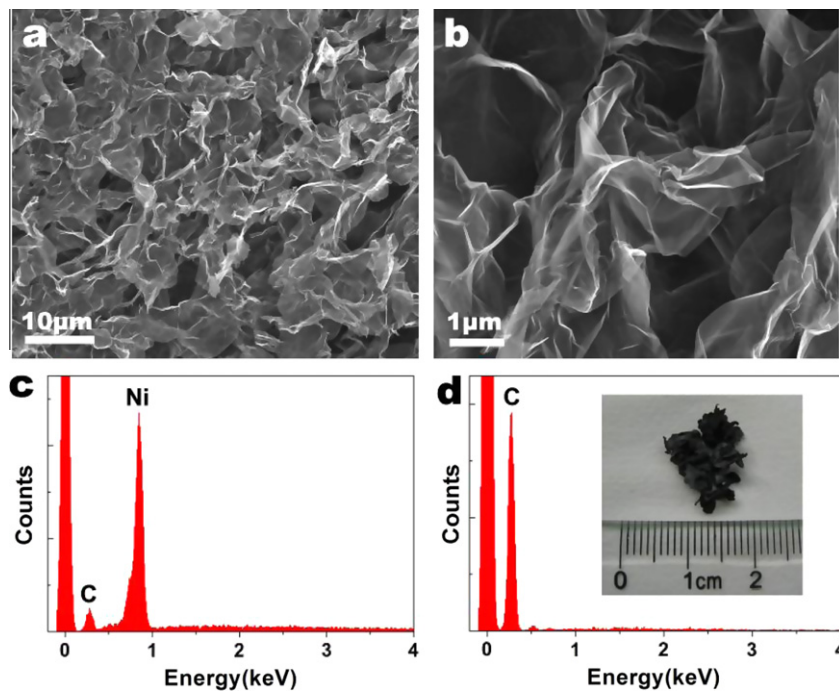


Fig. 2 – Characterization of graphene sheets after nickel particles were etched away. (a) and (b) low- and high-magnification SEM images of graphene sheets after the nickel particles were etched away by FeCl_3/HCl aqueous solution. (c) and (d): EDS spectra of the graphene samples shown in Fig. 1c and panel a, respectively, which indicate an efficient removal of nickel by etching. Inset of (d) is an optical image of the graphene sample after nickel particles were etched away.

the purified samples are free of nickel impurity. Inset of Fig. 2d shows an optical image of the graphene sample after nickel particles were removed. Typically, about 5 mg of pure graphene sheets were obtained from 200 mg of nickel particles within a CVD growth time of 5 min, which represents a growth yield of about 2.5 wt.%. It is worth noting that the amount of graphene can be easily scaled up for future appli-

cations by increasing the amount of nickel particles, and a continuous production of graphene can be expected by using the methods for CVD growth of CNTs proposed in references [38,39].

It is well known that the electronic properties of graphene sheets strongly depend on their number of layers and quality [2]. To evaluate the number of layers and quality of the ob-

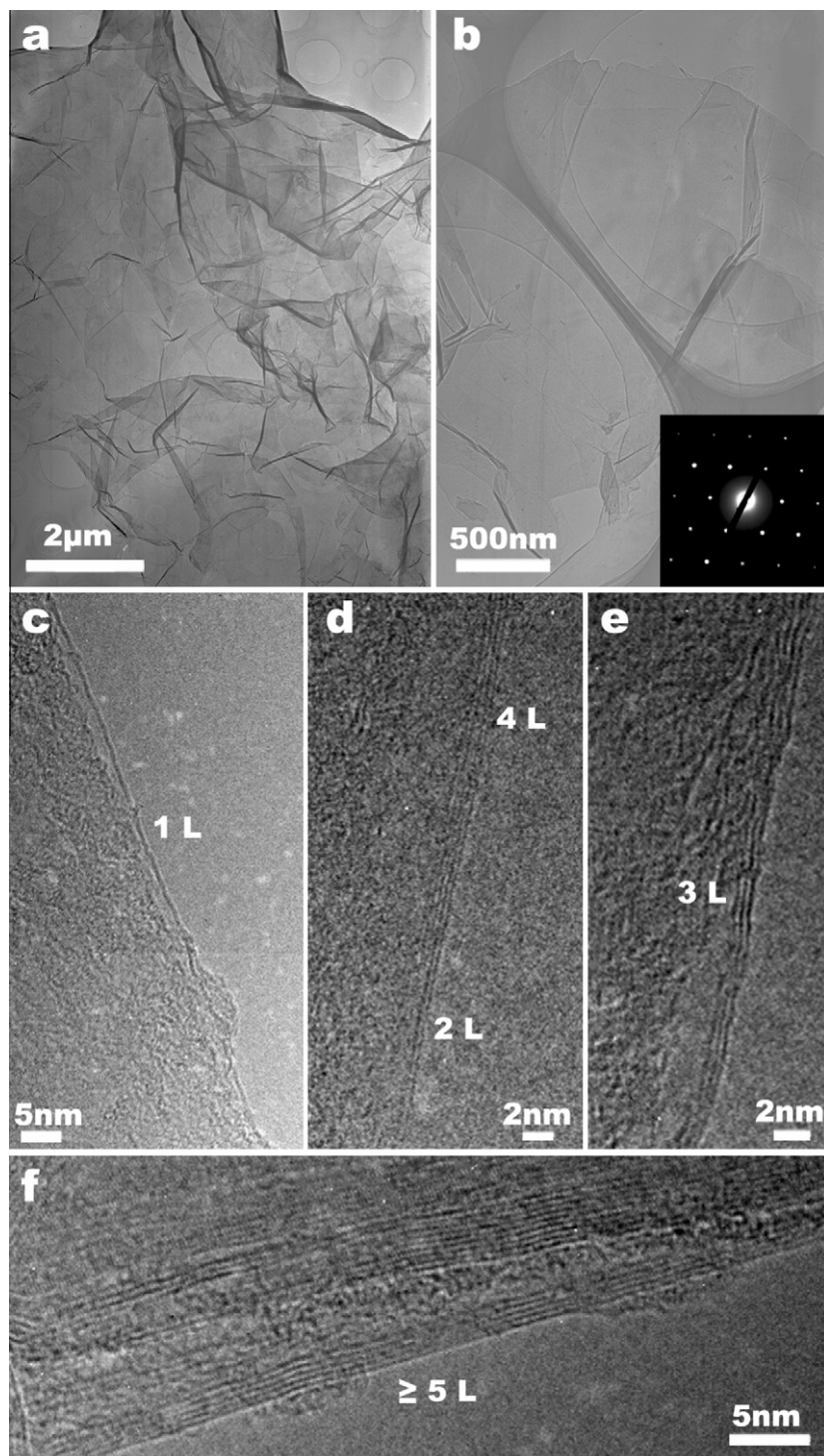


Fig. 3 – TEM characterizations of the CVD-grown graphene. (a) Low-magnification TEM image of graphene, showing a crumpled morphology with many wrinkles. (b) TEM image of an individual graphene sheet with a smooth surface. The electron diffraction of the graphene sheet is shown as an inset, indicating the excellent crystallinity of the sample. (c)–(f) HRTEM images of the edges of the graphene sheets with one (c), two and four (d), three (e), five or more (f) layers.

tained graphene sheets, we performed TEM measurements on the purified graphene (Fig. 3). As shown in Fig. 3a, most of the graphene sheets are crumpled with many ripples and wrinkles on their surface. We suggest that some of these wrinkles were formed during growth (Fig. 1b), and some were attributed to the collapse of graphene sheets after the removal of nickel particles. However, it is worth noting that there are small smooth regions in these big sheets. We also observed some individual small graphene sheets with smooth surface (Fig. 3b), which may be grown directly during the CVD process and come from the wrinkle-free regions in a large sheet because of the breaking of large sheets during sonication. The electron diffraction reveals a well-defined hexagonal pattern from the threefold symmetry arrangement of carbon atoms, indicating the excellent crystallinity of the graphene sheets obtained (Fig. 3b). As previously reported, suspended graphene films are usually folded at their edges, which allows for the cross-section view of graphene and direct identification of the number of layers accurately by using high-resolution TEM (HRTEM) [24,40]. Extensive HRTEM observations reveal that most of the graphene sheets have a thickness of 1–5 layers, although thick sheets with more than 5 layers were also occasionally observed (Fig. 3c–f). It is known that a long time of sonication of graphite in NMP may produce graphene [17]. In order to rule out this possibility, we also used ethanol for TEM specimen preparation. It is worth noting that no detectable difference in the structure of graphene obtained was found for these two solvents (Fig. S2). Therefore, we believe that the monolayer, bilayer and few-layer graphene sheets observed in TEM is due to growth but not sonication.

Raman spectroscopy is a powerful tool for identification of the detailed structure and quality of carbon materials. It has been reported that the number of layers, doping, strain, and defect characteristics of graphene can be easily identified by the profiles and positions of Raman peaks [40–45]. Fig. 4 shows the Raman spectra of the as-grown graphene on nickel particles and the graphene sheets after the removal of nickel particles. Similar to the Raman spectra of graphene prepared by micromechanical cleavage and flat substrate CVD [24,40], the two most intense Raman features of our graphene are the G band at $\sim 1580\text{ cm}^{-1}$ and the 2D band at $\sim 2660\text{ cm}^{-1}$. Moreover, most of the measured graphene sheets show a sharp and single Lorentzian 2D band with a full width at half maximum of $\sim 35\text{ cm}^{-1}$ and an intensity of several times stronger than the G band (the bottom spectra in Fig. 4), which are the fingerprints of monolayer graphene. This indicates that there are a high percentage of monolayer graphene in the grown material. In addition, it is worth noting that, different from the Raman spectra of graphene prepared by micromechanical cleavage, the 2D band of our graphene with different layers exhibits a symmetrical lineshape, although it upshifts and becomes broad with increasing the number of layers. As reported previously, the symmetrical lineshape of bilayer and few-layer graphene may be attributed to the absence of electronic coupling between graphene layers without AB stacking [24,46]. We consider that it is more possible in our case to get bilayer and few-layer graphene sheets without AB stacking order because of their curved structure and the presence of strain. As suggested before, these incommensurate

few-layer graphene sheets have unique electronic properties different from commensurate ones [47–49].

Moreover, the graphene sheets prepared on nickel particles show a very low intensity of disorder-induced D band ($\sim 1330\text{ cm}^{-1}$), with intensity ratio of D to G band varying from 0.02 to 0.2, strongly indicating their high quality. More importantly, only a slight increase of D band intensity is observed for the purified graphene (Fig. 4b), possibly due to the collapse and breaking of graphene films during the etching treatment. Therefore, it is reasonable to suggest that the purified graphene after the removal of nickel particles almost remain the high quality of the as-grown graphene. The high quality of the purified graphene can be further confirmed by its high thermal stability, with T_{max} (temperature corresponding to the highest combustion rate) of $\sim 800\text{ }^{\circ}\text{C}$ (Fig. S3, TG/DTG curves), which is higher than those of graphene prepared by hydrogen arc discharge exfoliation ($\sim 600\text{ }^{\circ}\text{C}$) [50].

Fig. 5 shows the typical I–V characteristics of the purified graphene sheets measured at ambient condition. Raman analyses indicate that the measured graphene sheets are few-layer graphene (Fig. S4). The sheet resistance of the individual graphene sheet in Fig. 5a is estimated to be $\sim 8.5\text{ k}\Omega$ per square from Fig. 5b, while the device with two or more graph-

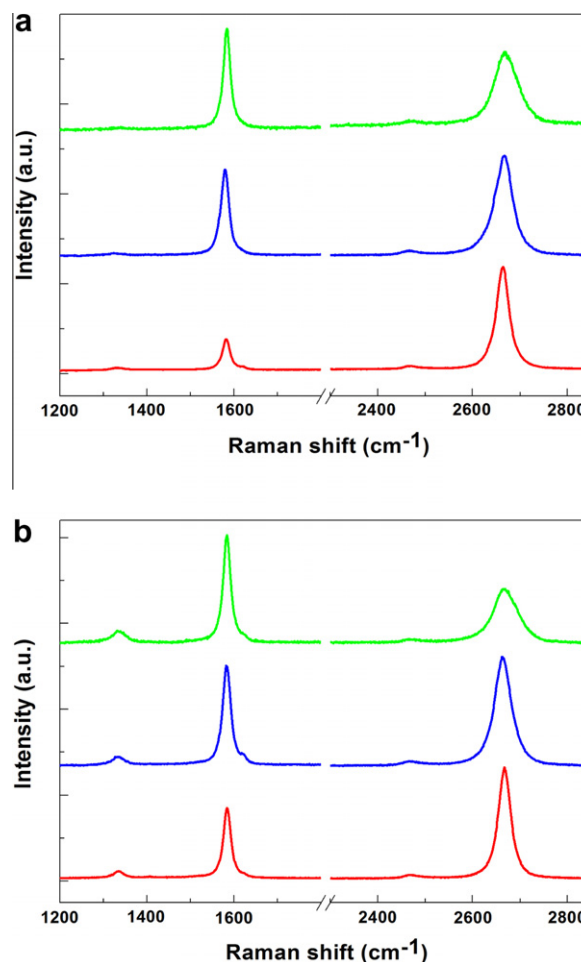


Fig. 4 – Typical Raman spectra of (a) as-grown and (b) purified graphene sheets.

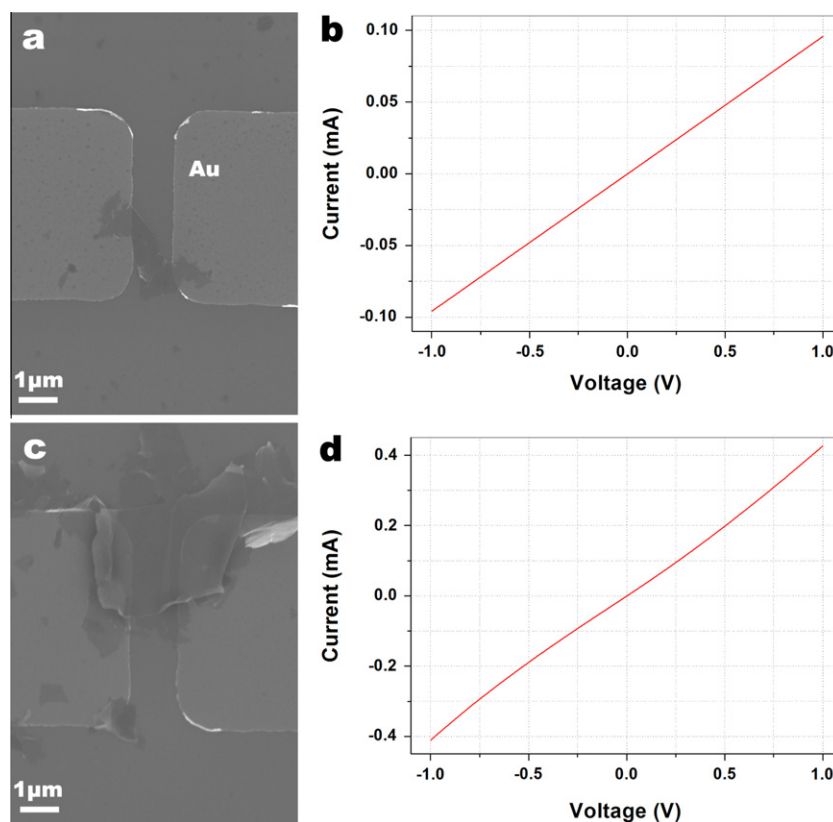


Fig. 5 – Electrical conductivity measurements of the purified graphene sheets. (a) and (b) SEM image and *I*-*V* curve of an individual graphene sheet. (c) and (d) SEM image and *I*-*V* curve of overlapped graphene sheets.

ene sheets overlapping together in Fig. 5c shows a sheet resistance of ~ 6.6 k Ω per square (Fig. 5d). The low sheet resistance measured in our graphene samples confirms the high quality of the graphene sheets grown on nickel particles.

4. Conclusions

We have proposed a CVD for bulk growth of high quality mono- to few-layer graphene sheets on nickel particles. A graphene yield of about 2.5% of the weight of nickel particles was achieved, within a growth time of 5 min. Interestingly, many suspended graphene films were prepared during this process, which bridged across nearby nickel grains. Moreover, the nickel particles can be removed effectively by a simple FeCl_3/HCl treatment without degradation of the quality of the graphene sheets. The purified graphene sheets exhibit a high quality with excellent crystallinity, low electrical resistance and high oxidation resistance temperature. Our results open up the possibility for the large-scale production of high quality graphene sheets, which may facilitate a wide range of applications of graphene, including composites, energy storage, transparent conductive films, field emitters, etc.

Acknowledgements

This work was supported by National Science Foundation of China (Nos. 509,21,004, 508,72,136 and 509,72,147) and Chinese Academy of Sciences (No. KJ9X2-YW-231).

Appendix A. Supplementary data

Supplementary data associated with this article can be found, in the online version, at [doi:10.1016/j.carbon.2010.05.052](https://doi.org/10.1016/j.carbon.2010.05.052).

REFERENCES

- [1] Novoselov KS, Geim AK, Morozov SV, Jiang D, Zhang Y, Dubonos SV, et al. Electric field effect in atomically thin carbon films. *Science* 2004;306(5296):666–9.
- [2] Geim AK, Novoselov KS. The rise of graphene. *Nat Mater* 2007;6(3):183–91.
- [3] Geim AK. Graphene: Status and prospects. *Science* 2009;324(5934):1530–4.
- [4] Novoselov KS, Jiang D, Schedin F, Booth TJ, Khotkevich VV, Morozov SV, et al. Two-dimensional atomic crystals. *P Natl Acad Sci USA* 2005;102(30):10451–3.
- [5] Novoselov KS, Geim AK, Morozov SV, Jiang D, Katsnelson MI, Grigorieva IV, et al. Two-dimensional gas of massless Dirac fermions in graphene. *Nature* 2005;438(7065):197–200.
- [6] Zhang YB, Tan YW, Stormer HL, Kim P. Experimental observation of the quantum Hall effect and Berry's phase in graphene. *Nature* 2005;438(7065):201–4.
- [7] Bolotin KI, Sikes KJ, Jiang Z, Klima M, Fudenberg G, Hone J, et al. Ultrahigh electron mobility in suspended graphene. *Solid State Commun* 2008;146(9–10):351–5.
- [8] Wu ZS, Pei SF, Ren WC, Tang DM, Gao LB, Liu BL, et al. Field emission of single-layer graphene films prepared by electrophoretic deposition. *Adv Mater* 2009;21(17):1756–60.

- [9] Wang DW, Li F, Zhao JP, Ren WC, Chen ZG, Tan J, et al. Fabrication of graphene/polyaniline composite paper via in situ anodic electropolymerization for high-performance flexible electrode. *ACS Nano* 2009;3(7):1745–52.
- [10] Wang X, Zhi LJ, Mullen K. Transparent, conductive graphene electrodes for dye-sensitized solar cells. *Nano Lett* 2008;8(1):323–7.
- [11] Dikin DA, Stankovich S, Zimney EJ, Piner RD, Dommett GHB, Evmenenko G, et al. Preparation and characterization of graphene oxide paper. *Nature* 2007;448(7152):457–60.
- [12] Stankovich S, Dikin DA, Piner RD, Kohlhaas KA, Kleinhammes A, Jia Y, et al. Synthesis of graphene-based nanosheets via chemical reduction of exfoliated graphite oxide. *Carbon* 2007;45(7):1558–65.
- [13] Wu ZS, Ren WC, Gao LB, Liu BL, Jiang CB, Cheng HM. Synthesis of high-quality graphene with a pre-determined number of layers. *Carbon* 2009;47(2):493–9.
- [14] Li D, Muller MB, Gilje S, Kaner RB, Wallace GG. Processable aqueous dispersions of graphene nanosheets. *Nat Nanotech* 2008;3(2):101–5.
- [15] Li XL, Zhang GY, Bai XD, Sun XM, Wang XR, Wang E, et al. Highly conducting graphene sheets and Langmuir-Blodgett films. *Nat Nanotech* 2008;3(9):538–42.
- [16] Hernandez Y, Nicolosi V, Lotya M, Blighe FM, Sun ZY, De S, et al. High-yield production of graphene by liquid-phase exfoliation of graphite. *Nat Nanotech* 2008;3(9):563–8.
- [17] Khan U, O'Neill A, Lotya M, De S, Coleman JN. High-concentration solvent exfoliation of graphene. *Small* 2010;6(7):864–71.
- [18] Berger C, Song ZM, Li XB, Wu XS, Brown N, Naud C, et al. Electronic confinement and coherence in patterned epitaxial graphene. *Science* 2006;312(5777):1191–6.
- [19] Berger C, Song ZM, Li TB, Li XB, Ogbazghi AY, Feng R, et al. Ultrathin epitaxial graphite: 2D electron gas properties and a route toward graphene-based nanoelectronics. *J Phys Chem B* 2004;108(52):19912–6.
- [20] Sutter PW, Flege JI, Sutter EA. Epitaxial graphene on ruthenium. *Nat Mater* 2008;7(5):406–11.
- [21] Dato A, Radmilovic V, Lee ZH, Phillips J, Frenklach M. Substrate-free gas-phase synthesis of graphene sheets. *Nano Lett* 2008;8(7):2012–6.
- [22] Yu QK, Lian J, Siriponglert S, Li H, Chen YP, Pei SS. Graphene segregated on Ni surfaces and transferred to insulators. *Appl Phys Lett* 2008;93(11):113103.
- [23] Chae S, Gunes F, Kim K, Kim E, Han G, Kim S, et al. Synthesis of large-area graphene layers on poly-nickel substrate by chemical vapor deposition: wrinkle formation. *Adv Mater* 2009;21(22):2328–33.
- [24] Reina A, Jia XT, Ho J, Nezich D, Son HB, Bulovic V, et al. Large area, few-layer graphene films on arbitrary substrates by chemical vapor deposition. *Nano Lett* 2009;9(1):30–5.
- [25] Kim K, Zhao Y, Jang H, Lee S, Kim J, Ahn J, et al. Large-scale pattern growth of graphene films for stretchable transparent electrodes. *Nature* 2009;457(7230):706–10.
- [26] De Arco LG, Zhang Y, Kumar A, Zhou CW. Synthesis, transfer, and devices of single- and few-layer graphene by chemical vapor deposition. *IEEE Trans Nanotechnol* 2009;8(2):135–8.
- [27] Pollard AJ, Nair RR, Sabki SN, Staddon CR, Perdigo LMA, Hsu CH, et al. Formation of monolayer graphene by annealing sacrificial nickel thin films. *J Phys Chem C* 2009;113(38):16565–7.
- [28] Alfonso Reina ST, Xiaoting Jia, Sreekar Bhaviripudi, Mildred S. Dresselhaus, Juergen A. Growth of large-area single- and bilayer graphene by controlled carbon precipitation on polycrystalline Ni surfaces. *Nano Res* 2009;2(6):509–16.
- [29] Mun JH, Hwang C, Lim SK, Cho BJ. Optical reflectance measurement of large-scale graphene layers synthesized on nickel thin film by carbon segregation. *Carbon* 2010;48(2):447–51.
- [30] Wei DC, Liu YQ, Wang Y, Zhang HL, Huang LP, Yu G. Synthesis of N-doped graphene by chemical vapor deposition and its electrical properties. *Nano Lett* 2009;9(5):1752–8.
- [31] Li X, Cai W, An J, Kim S, Nah J, Yang D, et al. Large-area synthesis of high-quality and uniform graphene films on copper foils. *Science* 2009;324(5932):1312–4.
- [32] Li X, Cai W, Colombo L, Ruoff RS. Evolution of graphene growth on Ni and Cu by carbon isotope labeling. *Nano Lett* 2009;9(12):4268–72.
- [33] Levendoff MP, Ruiz-Vargas CS, Garg S, Park J. Transfer-free batch fabrication of single layer graphene transistors. *Nano Lett* 2009;9(12):4479–83.
- [34] Li XS, Zhu YW, Cai WW, Borysiak M, Han BY, Chen D, et al. Transfer of large-area graphene films for high-performance transparent conductive electrodes. *Nano Lett* 2009;9(12):4359–63.
- [35] Vijayaraghavan A, Blatt S, Weissenberger D, Oron-Carl M, Hennrich F, Gerthsen D, et al. Ultra-large-scale directed assembly of single-walled carbon nanotube devices. *Nano Lett* 2007;7(6):1556–60.
- [36] Vijayaraghavan A, Sciascia C, Dehm S, Lombardo A, Bonetti A, Ferrari AC, et al. Dielectrophoretic assembly of high-density arrays of individual graphene devices for rapid screening. *ACS Nano* 2009;3(7):1729–34.
- [37] Du X, Skachko I, Barker A, Andrei EY. Approaching ballistic transport in suspended graphene. *Nat Nanotech* 2008;3(8):491–5.
- [38] Cheng HM, Li F, Su G, Pan HY, He LL, Sun X, et al. Large-scale and low-cost synthesis of single-walled carbon nanotubes by the catalytic pyrolysis of hydrocarbons. *Appl Phys Lett* 1998;72(25):3282–4.
- [39] Mora E, Tokune T, Harutyunyan AR. Continuous production of single-walled carbon nanotubes using a supported floating catalyst. *Carbon* 2007;45(5):971–7.
- [40] Ferrari AC, Meyer JC, Scardaci V, Casiraghi C, Lazzeri M, Mauri F, et al. Raman spectrum of graphene and graphene layers. *Phys Rev Lett* 2006;97(18):187401.
- [41] Ferrari AC. Raman spectroscopy of graphene and graphite: Disorder, electron-phonon coupling, doping and nonadiabatic effects. *Solid State Commun* 2007; 143(1–2):47–57.
- [42] Gupta A, Chen G, Joshi P, Tadigadapa S, Eklund PC. Raman scattering from high-frequency phonons in supported n-graphene layer films. *Nano Lett* 2006;6(12):2667–73.
- [43] Das A, Pisana S, Chakraborty B, Piscanec S, Saha SK, Waghmare UV, et al. Monitoring dopants by Raman scattering in an electrochemically top-gated graphene transistor. *Nat Nanotech* 2008;3(4):210–5.
- [44] Gao L, Ren W, Liu B, Saito R, Wu Z, Li S, et al. Surface and interference coenhanced Raman scattering of graphene. *ACS Nano* 2009;3(4):933–9.
- [45] Mohiuddin TMG, Lombardo A, Nair RR, Bonetti A, Savini G, Jalil R, et al. Uniaxial strain in graphene by Raman spectroscopy: G peak splitting, Gruneisen parameters, and sample orientation. *Phys Rev B* 2009;79(20):205433.
- [46] Lee DS, Riedl C, Krauss B, von Klitzing K, Starke U, Smet JH. Raman spectra of epitaxial graphene on SiC and of epitaxial graphene transferred to SiO₂. *Nano Lett* 2008;8(12):4320–5.
- [47] Dos Santos JMBL, Peres NMR, Castro AH. Graphene bilayer with a twist: Electronic structure. *Phys Rev Lett* 2007;99(25):256802.

- [48] Latil S, Henrard L. Charge carriers in few-layer graphene films. *Phys Rev Lett* 2006;97(3):036803.
- [49] Guinea F, Neto AHC, Peres NMR. Electronic states and Landau levels in graphene stacks. *Phys Rev B* 2006;73(24):245426.
- [50] Wu ZS, Ren WC, Gao LB, Zhao JP, Chen ZP, Liu BL, et al. Synthesis of graphene sheets with high electrical conductivity and good thermal stability by hydrogen arc discharge exfoliation. *ACS Nano* 2009;3(2):411–7.